Engineering with Computers (2000) 16: 16–23

Engineering with Computers

Modelling and Optimal Design of a Carbon Fibre Reinforced Composite Automotive Roof

M. E. Botkin

Vehicle Analysis and Dynamics Laboratory, GM R&D Center, Warren, MI, USA

Abstract. *Structural optimisation was used to carry out the design of an all-composite roof for a late model passenger car. CAD modelling procedures were used to develop the simplified geometric model of the composite roof starting with production CAD data and to create a shell mesh. The shell element roof model was combined with a beam model of the entire body in order to carry out the full-body optimisation. Optimisation results yielded a roof which was 71% lighter than the steel automotive roof, which weighed 94 lb (42.7 kg). Although this paper focuses on the use of commercially available software, it demonstrates a level of automation which is not typically used in the automotive industry.*

Keywords. Automeshing; Automotive; CAD Modelling; Composites; Finite Element Modelling; Optimisation

1. Introduction

In 1993 the U.S. Federal Government initiated a program administered by the Department of Commerce to develop highly fuel efficient cars of the future. PNGV (Partnership for a New Generation of Vehicles) was established between the Federal Government and the American automobile companies to carry out research and development in support of a goal to have 80 mpg family-sized vehicles in production by the year 2004 [1]. It was recognised that such highly efficient cars would need to be very lightweight; as much as 40% lighter than today's midsize cars. Because much of that mass is non-structural and perhaps can't be reduced, it was felt that the primary structure would need to be as much as 50% lighter than in today's cars. Mass reductions of that magnitude must be accomplished through the use of advanced, lightweight materials such as composites. Fibreglass reinforced composite bodies have been demonstrated [2], even to the extent of providing crashworthiness [3,4]. Because of the somewhat low mechanical properties, as compared to steel, of fibreglass composite materials, however, mass reductions of only 25–30% over steel are attainable. There have been only a limited number of demonstrations of the use of carbon fibre in automotive bodies, and none have been designed using finite element analysis, much less tested for structural performance [5,6]. However, carbon fibre has been proven for use in race cars [7] and exotic sports cars [8]. This paper provides a design methodology, including finite element analysis for realistic loading conditions, for a specific major body component. In addition, specific design studies show mass savings potential of 70%, although such predictions must be verified through physical testing.

Correspondence and offprint requests to: Prof M. E. Botkin, Vehicle Analysis and Dynamics Laboratory, GM Research and Development Centre, Warren, Michigan, 48090-9055, USA. Email: mark.e.botkin@gm.com

2. Modelling

2.1. Geometric Model

The geometric model for the composite roof was developed from production sheet metal parts so that the packaging constraints could be met as closely as possible. The sheet metal parts, however, contain considerable detail which is undesirable not only for composite parts, but also for mesh generation. In addition, the sheet metal model contains overlapping pieces and flanges with double thickness material. Figure 1 shows the geometric model for the sheet metal roof. The dark regions are actually the edges of numerous long, narrow surface patches.

Figure 2(a) is an enlargement of the 'B-pillar' region of the data. It was desired to *simplify* these data, i.e. reduce its geometrical complexity, but yet maintain the overall shape. This was done using the

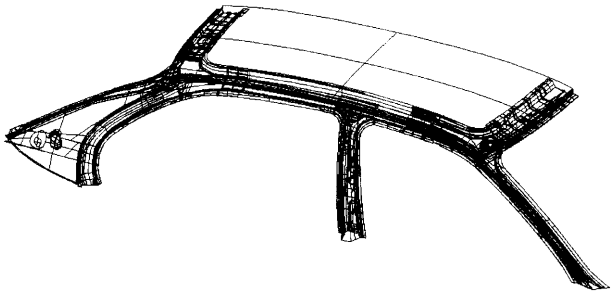

Fig. 1. Automotive roof (half) model.

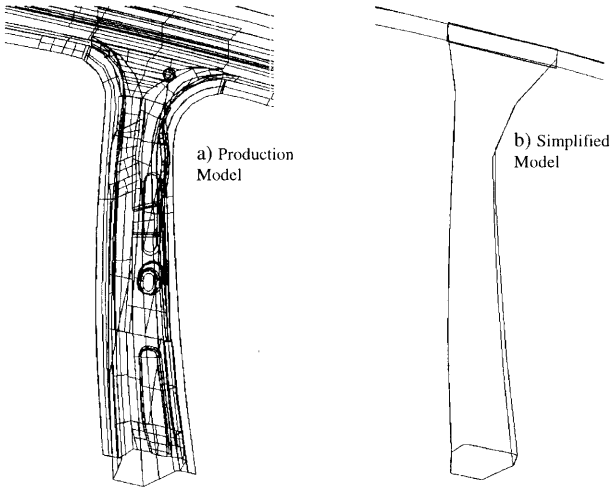

Fig. 2. B-pillar models.

advanced modelling capabilities of UNIGRAPHICS [9]. Special purpose surfacing operators allow new surfaces to be created using existing line or edge data. The resulting surfaces are large, high-degree patches which can be easily meshed using the fully-automatic quad-meshing capability. Figure 2(b) shows the new *B-pillar* created from selected edges of the original data. The surfacing technique requires *section* data and *guide* data. The section data, as its name implies, characterises the cross-section at several locations and the guide data generally provides orientation and scaling of the swept body and the direction of sweeping. These data are in the form of curves, and were obtained by *extracting* selected edge data from the original patches and concatenating the individual curves into continuous curves. Extending this same technique to the entire roof yields the model shown in Fig. 3. Obviously, this model does not contain many of the features of the original model, but it is considered to be suitable for creating an analysis and structural design model for this composite roof.

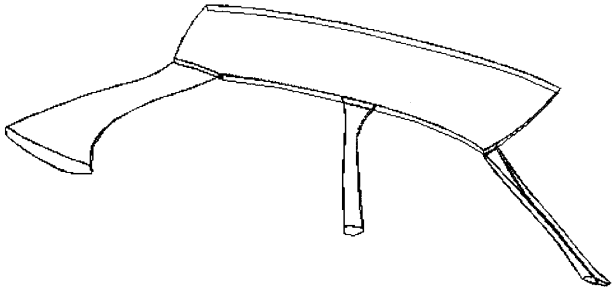

Fig. 3. Simplified roof model.

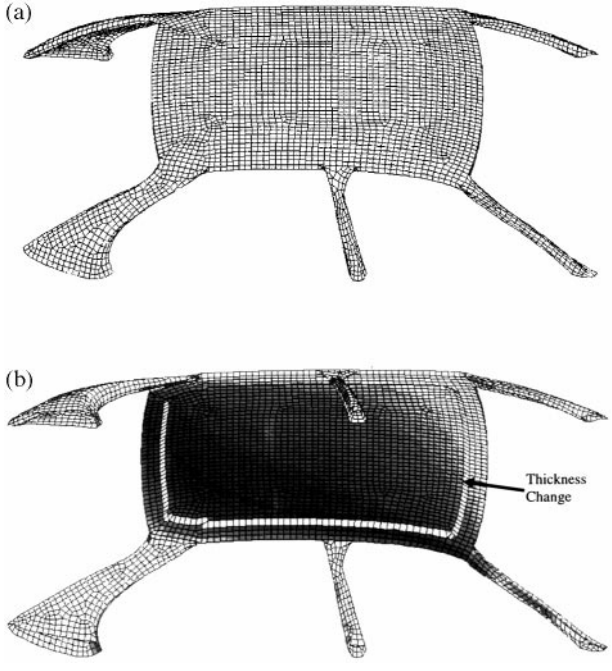

Fig. 4. (a) Roof finite element mesh (top view), (b) roof mesh (view from bottom).

2.2. Finite Element Analysis and Optimisation Model

The simplified geometrical model shown in Fig. 3 was used to automatically generate the finite element mesh using fully-automatic quadrilateral mesh generation; also a capability in UNIGRAPHICS. Figure 4(a) shows the completed mesh for the composite roof.

The seven large patches shown in Fig. 3 were meshed automatically with quads. To enforce continuity between patch boundaries, adjacent patches had to be manually identified before meshing a patch. The model in Fig. 4(a) is composed of 7044 quadrilateral shell elements. In addition, the roof panel – not including the pillars – is intended to be of a sandwich construction, i.e. polymer composite

skins with a core. For that reason, the quad mesh for the roof panel was *extruded* 25 mm to form a solid mesh containing 2428 hexahedral elements. Then, a shell mesh was placed on the interior of the solid core. The core is considered to be of a variable thickness, as can be see in Fig. 4(b), in which the thinner region is 10 mm. The resulting model contains 7409 nodes. Eleven orthotropic material property sets for carbon were identified, which will be described later in section 3, to provide for considerable design flexibility for the composite materials. Another isotropic material property set was defined for the core material. Local *material coordinate systems* were also defined for each pillar in which the longitudinal (*strong*) direction of the material is directed generally along the length of each pillar. In addition, the core material can be specified.

To complete the modelling task, the detailed shell model of Fig. 4 was merged with an optimised-for-composites vehicle body beam model [10] and is shown in Fig. 5.

Rigid links (Nastran RBE2 elements) were defined around the base of each pillar and attached to the closest nodes of the beam model. Non-structural masses also had to be defined to represent the mass of the front and back glass. Diagonal truss elements were also used to represent the shear stiffness of the glass. Although a molded composite structure would have better joint efficiencies than a sheet metal body, the existing joint coefficients (in the beam model) were used.

2.2.1. Static Load Cases

Several representative *static* load cases were considered: roof crush and 30 mph front barrier crash. Figure 6 shows the roof crush loading. The load is based on a total mass of 1023 kg, resulting in a total load of approximately 12 kN (1.5 times the vehicle mass). The design requirements for all of the static loads will be covered in the next section. Figure 7 shows a representative barrier impact load case. Unlike the roof crush load, the barrier loads are solved as *inertia relief* problems.

2.2.2. Typical Results

The original, *optimal* beam model yielded a first bending frequency of 27 Hz. The non-optimal combined model of Fig. 8 had a first bending of 23.6 Hz. Figure 9 shows a stress fringe plot for the roof crush load shown in Fig. 6, in which the maximum stresses (shown in dark grey and black) are below 200 Mpa (Von Mises). Figure 10 shows a fringe plot of a representative barrier load condition of Fig. 7, in which the Von Mises stresses are below 500 Mpa.

It should be pointed out that the stresses shown here do not accurately reflect the design limits as described in the next section, but merely give an indication of the relative influence of the loading cases.

3. Orthotropic Material Distribution

Material has been distributed in 11 distinct regions, as shown in Figs 11(a) and 11(b). Although an advantage of using composites is the ability to tailor the reinforcing material to meet the design requirements, it is desirable from a simplified manufacturing standpoint to reduce the number of different lay-ups. In general, Figs 11(a) and 11(b) show one

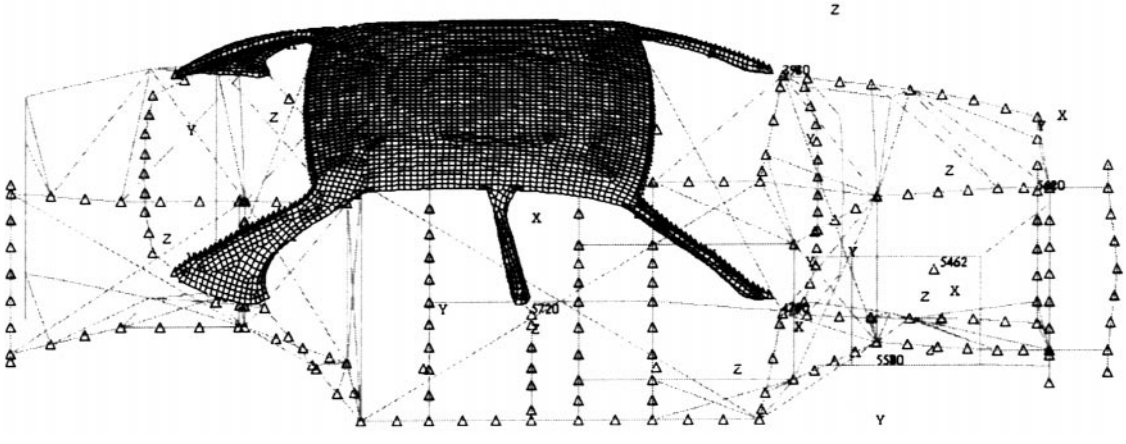

Fig. 5. Complete analysis/design model.

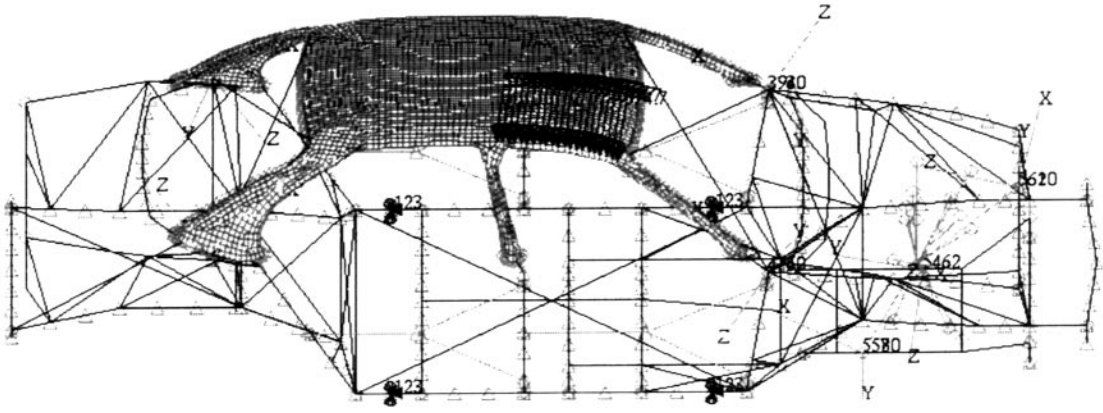

Fig. 6. Roof crush loading condition.

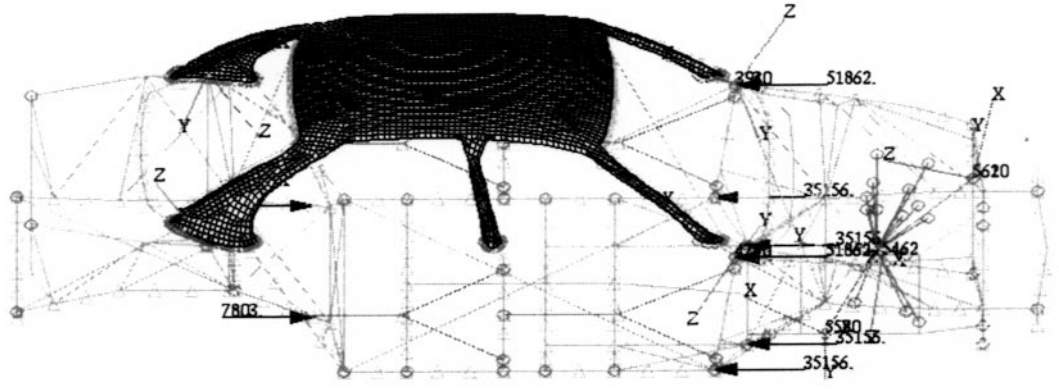

Fig. 7. Front barrier loading condition.

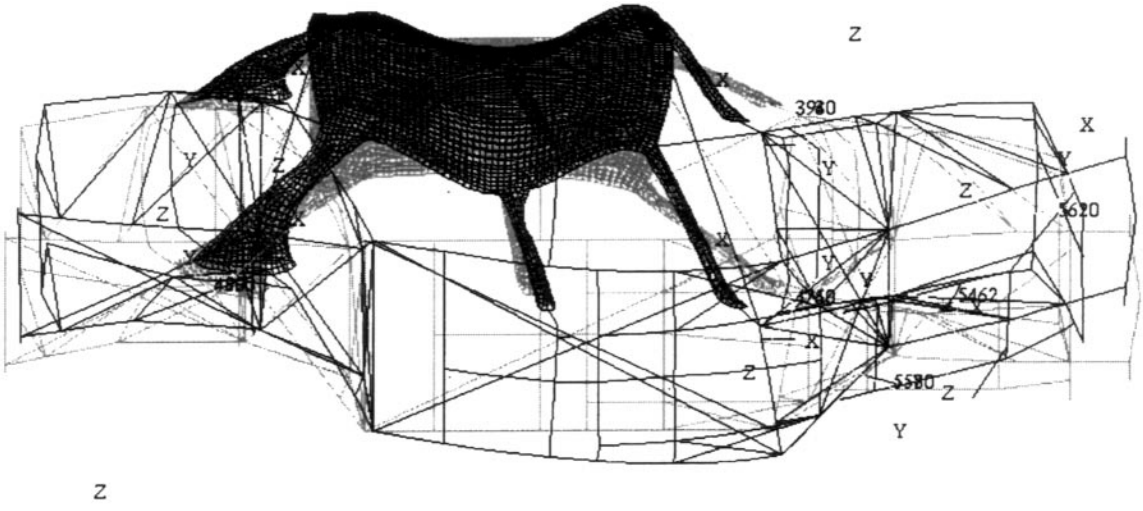

Fig. 8. First bending mode shape.

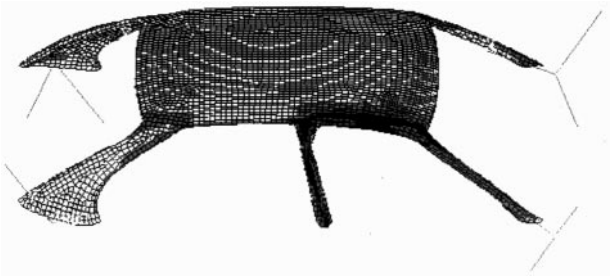

Fig. 9. Roof crush stress results.

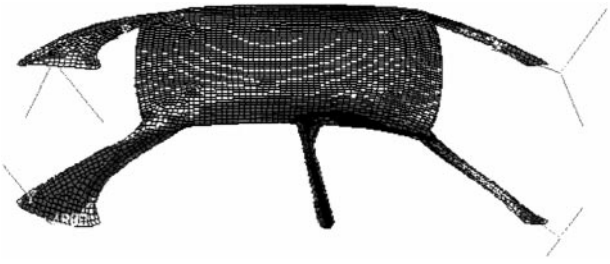

Fig. 10. Front barrier-load stress results.

region each for the A and B-pillars, two regions for the C-pillar, two large roof panel regions (inner & outer), an edge strip, and four regions surrounding the roof panels. In Section 5.1, a thickness design variable exists for each of the 11 regions shown in Fig. 11. In some cases, the inner panel (design variable #1 in Fig. 11(b)) was removed, resulting in 10 design variables. In one case, ply angles were considered as design variables for a total of 20 design variables.

4. Optimisation

The optimisation process minimises an objective function while constraining a number of response quantities. These functions and quantities are described below. Nastran *SOL*ution 200 [11] was used to carry out the optimisation studies. The approximation method used was *convex linearisation*, which is the most conservative of the approximation methods. Because of the difficulty of approximating the frequency and failure constraints, move limits of 10% were imposed on all design studies reported in the next section. Otherwise, all of the default optimisation parameters were utilised.

4.1. Objective Function

The objective function is the mass of the composite roof and the foam core. Nastran Sol 200 has an

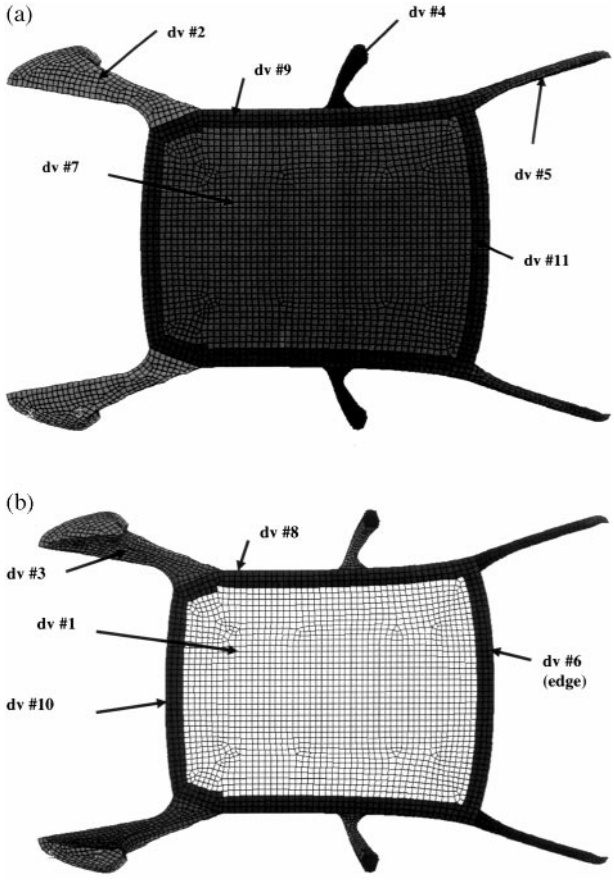

Fig. 11. Material distribution and design variables. (a) Topview, (b) bottom view.

option to use weight as an objective. This weight, however, is the complete weight of all structural elements. An alternative objective function was used which excluded the mass of the structural elements not associated with design variables in this study: $W(A) = A - 55.77$ in kg units, and includes approximately 3 kg of foam. A is the mass of the complete body.

4.2. Constraint Functions

Constraints are placed on the design to maintain a first bending frequency of 24 Hz, and maximum stress values are imposed for the *static* loading conditions. Since composite laminates fail differently than isotropic, metallic materials, an appropriate failure theory must be used. Nastran provides four theories, and the Hill theory (modified later by Tsai, and hence also sometimes known as the Tsai–Hill theory) [12] is commonly used to provide the failure index, f_i:

$$\frac{\sigma_1^2}{X^2} - \frac{\sigma_1\,\sigma_2}{X^2} + \frac{\sigma_2^2}{Y^2} + \frac{\tau_{12}^2}{S^2} = f_i \tag{1}$$

in which σ_1 is the stress component in the longitudinal direction, σ_2 is the stress in the transverse direction and τ_{12} is the shear stress. X is the longitudinal strength, and is equal to the tensile strength if σ_1 is positive and the compressive strength if σ_1 is negative. Y is the transverse strength, and uses the same rule as stated for X. S is the shear strength.

Another similar but different theory was developed by Hoffman [13]:

$$\left(\frac{1}{X_t} - \frac{1}{X_c}\right)\sigma_1 + \left(\frac{1}{Y_t} - \frac{1}{Y_c}\right)\sigma_2 + \frac{\sigma_1^2}{X_t\,X_c} + \frac{\sigma_2^2}{Y_t\,Y_c} + \frac{\tau_{12}^2}{S^2} - \frac{\sigma_1\,\sigma_2}{X_t\,X_c} = f_i \tag{2}$$

in which the t and c subscripts refer to tension and compression. Note that the Hoffman criterion gives a more rigorous treatment of compression and tensile properties, whereas the Hill equation uses one *or* the other.

As can be seen, these theories compare each stress component with each strength value individually. The material is considered to have failed if the failure index is greater than 1.0. For this study, a limiting value of 0.9 is used to include a safety factor. It should also be noted that f_i is a nonlinear function and, therefore, creates the potential of increasing the difficulty of solving the optimisation problem.

5. Optimisation Results

5.1. Design Studies

Several optimisation studies were carried out using material properties given in the Table 1. The properties are *actual measured* properties for carbon fibre composites made using a Resin Transfer Molding (RTM) process at General Motors. Row 1 is a unidirectional lay-up, and row 2 is a 0/90 stitched mat. Minimum gauge was taken to be 1.0 mm. Initial designs were chosen which were feasible, i.e. all responses were well within the allowable ranges. Figure 12 gives the results in terms of the mass of the roof, including the 3.0 kg foam core. Figure 13 shows the converged design variables for all four cases. A frequency constraint of 24 Hz was imposed, and all designs converged to an active frequency constraint as well as several active failure index constraints. Failure index constraints come from a static roof crush load case and a front barrier inertia

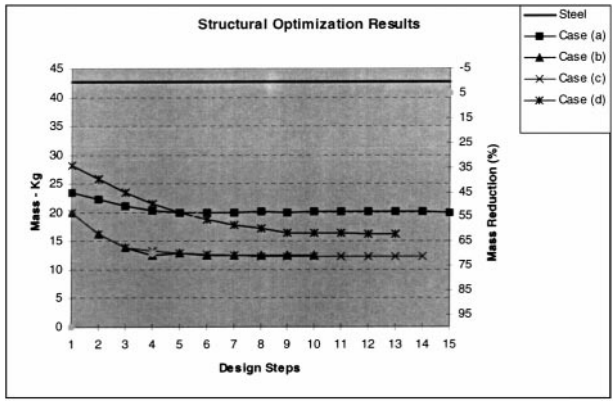

Fig. 12. Structural optimisation results.

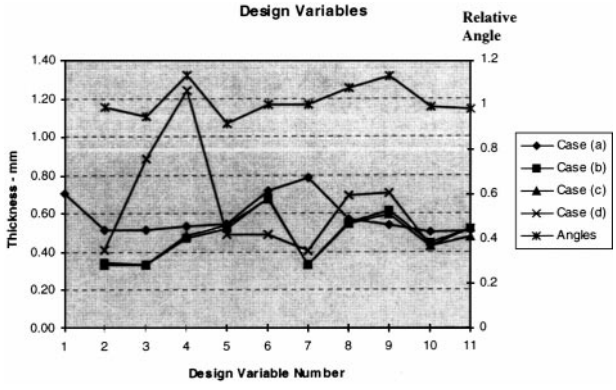

Fig. 13. Design variables.

Table 1. Composite material properties

Material type	E_1 (Mpa)	E_2 (Mpa)	μ	G (Mpa)	ρ (kg/mm^3)	X_t (Mpa)	X_c (Mpa)	Y_t (Mpa)	Y_c (Mpa)	S (Mpa)
Uni-directional carbon	130,000	9000	0.3	4800	1.50E-6	1630	840	34	110	60
(0/90) mat carbon	52,000	52,000	0.3	4200	1.43E-6	530	370	530	370	75
Tri-axial braid (0/–45/45)	60,000	9900	0.3	9510	1.50E-6	582	155	52	56	54
Foam core	20	20	–	4.63	8.1E-8	–	–	–	–	–

relief load condition. The Hoffman equation (Eq. (2)) was used for all studies. Rear barrier loads were not considered. Four cases are reported.

Case (a)
This case represents a complete *sandwich* construction using the material distributions shown in Fig. 11. A unidirectional lay-up of $(0/45/\text{-}45)_{sym}$ was used in all regions except the inner and outer roof panel. In the roof panels, the (0/90) mat was assumed. This case had 11 design variables (shown in Figs 11(a) and (b)) and 69 constraints. The design variables are the layer thickness of each material region with each layer being of equal thickness. This study yielded a 53% mass reduction over the production steel roof.

Case (b)
This case has the inner panel (and foam core) removed, with thickness-only design variables. Although it is generally felt that a sandwich construction is desirable for composites, a mass penalty is incurred since a *single* steel panel has been replaced by *two* composite panels. This case had 10 design variables as defined in Case (a) and 73 constraints. A mass reduction of 70% was obtained.

Case (c)
The inner panel (foam core) was removed (as in case (b)) with ply angle design variables. This case had 20 design variables and 73 constraints. Although this is a relatively unrealistic case, one can obtain some trends toward more favourable material angles. Converged ply-angle design variables are shown in Fig. 13 relative to 45°. It is interesting to note that the ply-angle design variables do not directly affect the mass, but rather affect the structural response. Then as the response improves, the optimiser reduces the mass further. A mass reduction of 71% over the steel roof was obtained. Due to the larger number of design variables, more iterations were required for convergence.

Case (d)
A commonly used automotive reinforcement type is the tri-axial braid. This case represents the use of braided material in all areas except the roof panel. Material properties for a $(0_{48k}/45_{12k}/-45_{12k})_{sym}$ carbon fibre braid are shown in Table 1 and were also measured. The 48k designation refers to the number of individual fibres per *tow*. The 48k carbon fibre product is lower cost than the 12k fibre product. As can be seen from the table, although the braid is desirable from manufacturing and cost points of view, the properties are generally lower. This is reflected in Fig. 12, in which it can be seen that a much heavier initial design had to be used to obtain a feasible initial design. The final design was also heavier than cases (b) and (c) at 62% mass reduction over steel. It can be seen in Fig. 13 that a much thicker B-pillar was produced. It is interesting to note that the ply-angle design variables have some of the same trends as the braid design variables, indicating a need for more fibres in the transverse direction for the B-pillar.

5.2. Limitations in Scope

It should be recognised that the optimised composite roof designs were compared with *actual*, non-optimised production steel roof structures. For that reason, the comparisons may not directly correspond, but merely give an indication of the mass savings potential of carbon fibre composites. Furthermore, the composite material layout was not intended to represent a finalised, production fabrication scheme. Manufacturing considerations regarding fabrication were not taken into account. That is, material lay-up in a region was considered to be independent of the lay-up in the adjacent region. Although each region possessed six layers of material, each layer *could* be composed of several physical plies of carbon fibre reinforcement due to the very small thickness of these plies. Therefore, there was the opportunity to create many more layers, and hence many more design variables, which could give rise to an even greater mass reduction.

Finally, design for crash and crush loads were handled only approximately. These load cases were designed to *avoid* failure, whereas in reality failure will occur resulting in a specified maximum displacement. Even if crash/crush analyses could be accomplished, it would be impractical to include them in a design loop. Therefore, designs for these loads are conservative.

6. Summary and Conclusions

This paper describes the modelling and design optimisation of an all-composite automotive roof structure. The geometric model was taken from the CAD data for a production steel roof. The original data were too detailed to be used directly for mesh generation. Simplification of the CAD data was accomplished through the use of surface modelling capabilities in UNIGRAPHICS. This new data were

then meshed using fully-automatic quad meshing techniques. The shell model of the roof was then combined with a beam model of the rest of the body in order to carry out a full-body optimisation study. Realistic analysis cases including frequency, barrier impact and roof crush were included in the optimisation studies. These studies included two different material systems and two different geometric-configuration concepts.

The studies show that large mass reductions, compared to steel, can be obtained using carbon fibre composites. All cases showed a minimum mass reduction of 53% for a configuration in which sandwich construction was used throughout the roof structure. The greatest mass reduction of 71% was obtained, however, when the roof panel was comprised of a single (not sandwich) carbon fibre panel. Another case, however, showed that this highest value of mass reduction potential was reduced to 63% when using a braided material due to the lower mechanical properties of a braid.

References

1. PNGV Home Page. (1997) http://www.ta.doc.gov/pngv
2. Bonnett, R.E. et al. (1995) Design of structural composites in a lightweight body structure. Proceedings of the 11th Annual ESD Advanced Composites Conference & Exhibition, Dearborn, MI, 75–86
3. Botkin, M.E., Fidan, S., Jeryan, R.A. (1997) Crashworthiness of a production vehicle incorporating a fiberglass reinforced composite front structure. SAE Paper No. 971522, 99–106
4. Wald, M. (1995) Solectria says car passed crash test. The New York Times, Wednesday November 22
5. Ashley, S. (1992) GM's ultralite is racing toward greater fuel efficiency. Mechanical Engineering, May, 64–67
6. Arneson, D., Marley, M. (1979) Detroit brings space age materials down to earth. Iron Age, April 9, 37–40
7. Browne, A.L. et al. (1996) A side impact test procedure for composite sandwich panels. Proceedings of the Society of Automotive Engineers Motorsports Engineering Conference, December 10–12
8. Ciferri, L. (1995) Stable mate: First drive! Ferrari F50. Autoweek, August 14, 14
9. Unigraphics II Finite Element Model Manual (1992) UG Finite Element Module Plus Operational Description, Release V9.0, Document MU2045
10. Bennett, J.A. et al. (1995) A multidisciplinary framework for preliminary vehicle design. Proceedings of the ICASE/NASA Langley Workshop on Multidisciplinary Design Optimization, Hampton, VA, 3–21
11. Moore, G.J. (1994) Design Sensitivity and Optimization, MSC/NASTRAN® User's Guide
12. Tsai, S.W. (1965) Strength Characteristics of Composite Materials. NASA CR-224
13. Narayanaswami, R., Adelman, H.M. (1977) Evaluation of the tensor polynomial and Hoffman strength theories for composite materials. Journal of Composite Materials, 11, 366–377